Electron Spin Coherence in Optically Excited States of Rare-Earth Ions for Microwave to Optical Quantum Transducers

Sacha Welinski,[1] Philip J. T. Woodburn,[2] Nikolai Lauk,[3] Rufus L. Cone,[2] Christoph Simon,[3] Philippe Goldner,[1] and Charles W. Thiel[2]

[1]*Université PSL, Chimie ParisTech, CNRS, Institut de Recherche de Chimie Paris, 11 rue Pierre et Marie Curie, 75005 Paris, France*
[2]*Department of Physics, Montana State University, Bozeman, Montana 59717, USA*
[3]*Institute for Quantum Science and Technology and Department of Physics and Astronomy, University of Calgary, Calgary AB T2N 1N4, Canada*

(Received 16 February 2018; published 17 June 2019)

Efficient and reversible optical to microwave transducers are required for entanglement transfer between superconducting qubits and light in quantum networks. Rare-earth-doped crystals with narrow optical and spin transitions are a promising system for enabling these devices. Current resonant transduction approaches use ground-state electron spin transitions that have coherence lifetimes often limited by spin flip-flop processes and spectral diffusion, even at very low temperatures. We investigate spin coherence in an optically excited state of an Er^{3+}: Y_2SiO_5 crystal at temperatures from 1.6 to 3.5 K for a low 8.7 mT magnetic field compatible with superconducting resonators. Spin coherence and population lifetimes of up to 1.6 μs and 1.2 ms, respectively, are measured by optically detected spin echo experiments. Analysis of decoherence processes suggest that ms coherence can be reached at lower temperatures for the excited-state spins, whereas ground-state spin coherence would be limited to a few μs due to resonant interactions with other Er^{3+} spins in the lattice and greater instantaneous spectral diffusion from the radio-frequency control pulses. We propose a quantum transducer scheme with potential for close to unity efficiency that exploits the advantages offered by spin states of the optically excited electronic energy levels.

DOI: 10.1103/PhysRevLett.122.247401

Rare-earth (RE)-doped crystals can exhibit long optical and spin coherence lifetimes at liquid helium temperatures that are promising for quantum technologies [1–3]. Long-lived quantum memories for light [4], entanglement storage [5], light-to-matter teleportation [6], and atomic-gas to crystal quantum state transfer [7] have all been demonstrated. These systems offer multimode storage [8,9] and high efficiency [10,11] with coherence lifetimes as long as hours [3], as well as the capability for signal processing of photonic quantum states [12]. Developments toward integrated and hybrid systems have also been reported using nanostructured materials [13,14], making RE-doped crystals a promising platform for solid-state quantum light-matter interfaces. RE ions with an odd number of electrons are particularly interesting since their strong magnetism allows efficient coupling to microwave photons. This could enable quantum-state transfer between superconducting qubits and light to build networks of quantum processors [15,16]. Strong coupling between superconducting resonators and RE ions has been demonstrated, and microwave to optical conversion has been investigated [17–20].

Using both optical and spin transitions requires strong coupling between light and microwaves. Ensembles of RE ions in crystals are generally employed to enhance the interaction with photons. While providing a number of advantages, ensembles also cause difficulties when considering optical to spin coherence transfer and undesired effects from ion-ion interactions. The weak optical oscillator strengths also limit addressable bandwidths for π pulses to less than 100 MHz; however, optical inhomogeneous linewidths are usually $\sim$1 GHz or larger [1], so that a majority of ions do not participate in the coherent excitation and are only "spectators."

If a resonant transduction protocol, such as Ref. [16], requires coherence to be stored in a superposition of the ground-state electron spin states, two undesirable effects can occur that have not been previously considered. First, the excitation can be incoherently transferred by fast spin flip flops, or spin diffusion, to other spins in the lattice, including spectator spins, resulting in decoherence and loss of the stored quantum state [21,22]. Second, to mitigate effects of inhomogeneous broadening on the achievable coherence time, a dynamical decoupling sequence should be applied; however, this requires drive pulses with bandwidths comparable to the spin inhomogeneous linewidths, which will also excite spectator spins since there is no correlation between optical and spin frequencies within their respective inhomogeneous linewidths. Since high-bandwidth control pulses will drive a large number of spectator spins, they can cause decoherence by instantaneous spectral diffusion (ISD) from long-range spin-spin interactions [19,23,24]. This is particularly important for

paramagnetic RE ions since they exhibit significant spin-spin interactions even for concentrations as low as 10 ppm [25]. Consequently, this source of decoherence often cannot be eliminated by reducing ion concentration without also reducing optical absorption and limiting device efficiency.

We propose to circumvent these limitations of resonant transduction approaches by using spin transitions for optically excited electronic states. Because excited ions' spins are not resonant with the larger number of spectator spins, decoherence due to flip-flop processes are significantly reduced. Furthermore, only optically excited spins are resonant with the microwave fields, avoiding excitation of spectator spins by control pulses and reducing ISD to the lowest possible extent. While this scheme is limited by the excited-state population lifetime $T_{1,\mathrm{opt}}$, this can be longer than ms for RE ions, meeting the requirements for microwave-optical transduction protocols. A particularly favorable ion is erbium with typical excited-state lifetimes of ~10 ms for the $^4I_{13/2}$ level [26]. This 1.5 μm telecom wavelength transition has attracted strong interest for building fiber-based quantum networks and transducers [18,20,27]. Here, we investigate electron spin coherence in the excited state of an Er^{3+} -doped Y_2SiO_5 crystal and observe excited-state electron spin echoes for RE ions. We also present an excited-state transduction protocol that can approach unity efficiency.

The work here focuses on the effects of spin flip flops on spin coherence, spin-state lifetimes, and efficiency of resonant transduction approaches such as proposed by O'Brien *et al.* [16]. While off-resonance transduction schemes, as proposed by Williamson *et al.* [15], are not directly affected by optical or spin coherence lifetimes, they can still be affected by spin flip flops if spectral diffusion becomes comparable to the spin inhomogeneous broadening or if spin-state lifetimes become comparable to the microwave or optical cavity lifetimes. The existing theory for the off-resonant approach assumes that spin states and transition frequencies are fixed for all ions in the ensemble during the timescale of the transduction process to obtain analytical solutions for the transduction efficiency [15]. Hence, the effect of spin flip flops cannot be analyzed within the existing theory beyond a general observation that fluctuating spin states and frequencies will act to reduce transduction efficiency. It is not possible to say whether the effects are significant for practical conditions without expanding the theory to include spin dynamics.

Coherent Raman heterodyne scattering (RHS) [28] experiments were performed for the three-level schemes shown in Fig. 1. This method employs a radio-frequency (rf) field resonant with Zeeman transition $|1\rangle \leftrightarrow |2\rangle$ or $|3\rangle \leftrightarrow |4\rangle$ to create a ground- or excited-state electron spin coherence [Fig. 1(a)]. A resonant laser beam drives the optical transition $|1\rangle \leftrightarrow |3\rangle$ or $|1\rangle \leftrightarrow |4\rangle$. The combined optical and rf coherences then induce coherence on the other optical transition $|2\rangle \leftrightarrow |3\rangle$ or $|1\rangle \leftrightarrow |3\rangle$ that then interferes with the laser field, producing a beat note at the $|1\rangle \leftrightarrow |2\rangle$ or $|3\rangle \leftrightarrow |4\rangle$ frequencies that is detected using a photodiode.

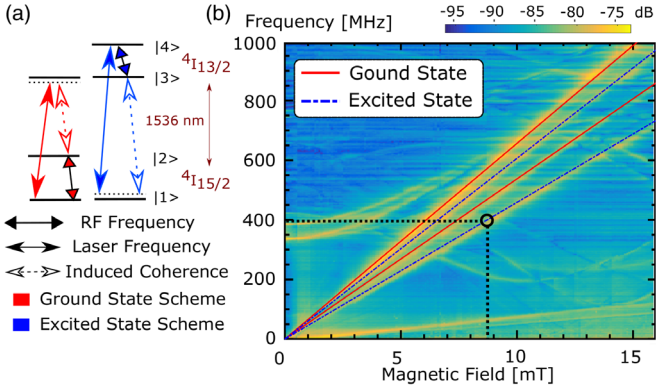

FIG. 1. (a) Energy levels of Er^{3+} and RHS schemes for ground- and excited-state spin coherence studies ($|1\rangle \leftrightarrow |2\rangle$ and $|3\rangle \leftrightarrow |4\rangle$ are electron spin transitions). (b) The RHS measurements at 3 K on Er^{3+} at site 1 of Y_2SiO_5. Lines: fitted Zeeman transition frequencies for zero-nuclear-spin Er^{3+} isotopes. Black circle and dashed lines: spin echo experimental condition.

A 50 ppm Er^{3+} -doped Y_2SiO_5 sample grown by Scientific Materials Corp. was cut along the three dielectric axes: b, D_1, D_2 [29] and mounted in an Oxford Optistat helium cryostat with a magnetic field applied along D_1 using a Helmholtz coil. Er^{3+} can substitute for Y^{3+} at two inequivalent crystallographic sites (denoted 1 and 2). An external-cavity diode laser was set at 1536.49 nm (vacuum) in resonance with the transition between the lowest levels of the $^4I_{15/2}$ and $^4I_{13/2}$ multiplets for ions at site 1 [26]. The laser was amplified and then focused into the crystal with propagation along the b axis and polarization along the D_2 axis. The laser produced nearly equal populations in the ground and excited states over ~1 MHz bandwidth. Optical pumping also induced population differences within the ground- and excited-state Zeeman sublevels necessary to detect spin coherence with RHS. Transmitted light was detected by a 1 GHz ac-coupled photoreceiver. The rf pulses with magnetic field amplitudes of several Gauss were applied along b through an rf strip waveguide next to the crystal surface.

Figure 1(b) shows RHS spectra for frequencies up to 1 GHz as a function of magnetic field strength. In these experiments, an rf spectrum analyzer generated the rf excitation and analyzed the photoreceiver signal (see the Supplemental Material [30]). The four lines observed in Fig. 1(b) correspond to electron-spin transitions for the ground and excited states of Er^{3+} isotopes with zero nuclear spin, deduced from the magnetic field direction and known $\mathbf{g}$ tensors [37,38]. Two transitions are observed for each state since the magnetic field was not exactly parallel to D_1, resulting in two inequivalent subgroups for each site. The corresponding effective ground-state

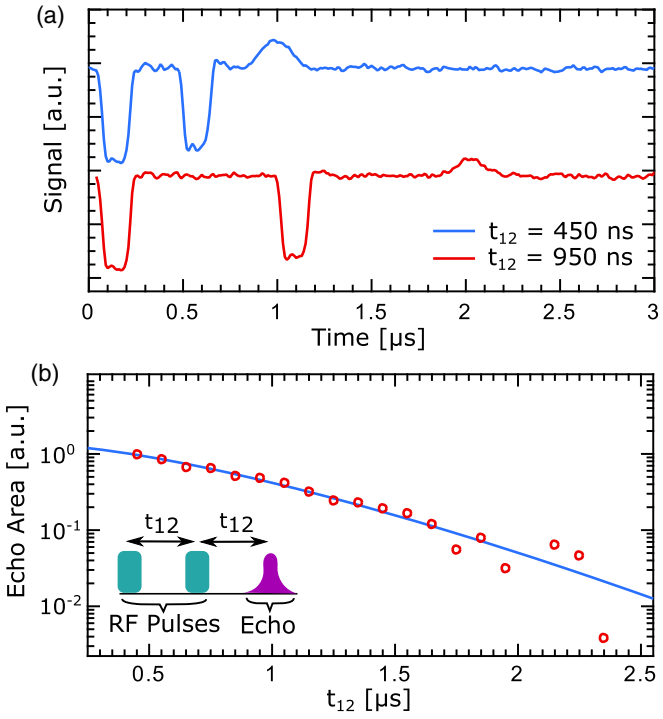

FIG. 2. (a) Optically detected electron spin echoes in the $^4I_{13/2}$ excited state for different pulse delays with $T = 1.9$ K and $B = 8.7$ mT. (b) Measurement (circles) and fit (line) of echo decay at 1.9 K, giving $T_2 = 1.6 \pm 0.2$ μs and $x = 1.4 \pm 0.2$. Inset: rf pulse sequence.

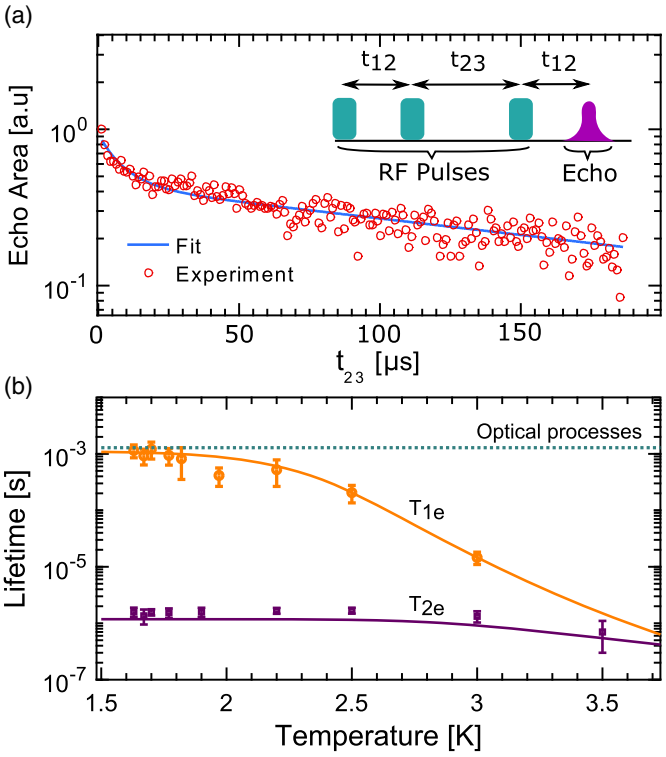

FIG. 3. (a) Excited-state stimulated spin echo decay measured at 2.5 K (circles) and fit to the spectral diffusion model (line, see text). Inset: rf pulse sequence. (b) Experimental coherence (squares) and population lifetimes (circles) as a function of temperature. Dotted line: population lifetime deduced from the sum of optical emission and excitation rates; solid lines: calculated and fitted curves (see text).

values g_g are 4.75 and 3.85 (± 0.3), and the excited-state values g_e are 4.35 and 3.27 (± 0.3), depicted in Fig. 1(b). All spin transitions exhibited linewidths of $\sim$10 MHz, similar to those previously reported [20,37]. The linewidths did not vary significantly with magnetic field strength, indicating that the spin-transition broadening does not arise from inhomogeneity in the **g** tensors or the field. Weaker transitions with complex field dependence are also visible in Fig. 1(b) and are attributed to hyperfine transitions of the $^{167}Er^{3+}$ isotope ($I = 7/2$, abundance 22.9%).

Excited-state spin echoes were measured using rf pulses generated by a gated source. The photoreceiver signal was amplified, filtered, and down mixed with a local oscillator (see the Supplemental Material [30]). A dc magnetic field of 8.7 mT was applied along the same orientation as in the cw experiments, and a frequency of 400 MHz was used to study the excited-state transition [Figs. 1(a) and 1(b)] for temperatures from 1.6 to 3.5 K.

The two-pulse echo signal is shown in Fig. 2(a) for two different delays between excitation pulses. Pulse lengths of 150 ns maximized the echo signal. Detected echoes had a π phase shift relative to the excitation pulses, confirming that the entire sequence was phase coherent. The cw laser excitation created a large excited-state population that produced strong echo signals. The integrated echo signal decay was measured as a function of the delay between the pulses [Fig. 2(b)] and fitted with a Mims function [39]

$$A(t_{12}) = A \exp\left[-(2t_{12}/T_{2e})^x\right], \tag{1}$$

where T_{2e} is the $1/e$ coherence lifetime and t_{12} is the delay between pulses. The extracted T_{2e} at 1.9 K was 1.6 ± 0.2 μs (200 kHz homogeneous linewidth), with $x = 1.4 \pm 0.2$. The nonexponential behavior arises from spectral diffusion [39] attributed to interactions with Er^{3+} spins in the lattice. The effect of ^{89}Y nuclear spins is expected to be much weaker because of their small magnetic moment and slow flip rates [21].

To probe the decoherence mechanisms, we measured three-pulse stimulated spin echoes using the pulse sequence shown in Fig. 3(a). Stimulated echo measurements allow spin relaxation and spectral diffusion dynamics to be studied over the timescale of T_1, whereas two-pulse echoes are limited to the much shorter T_2 timescale [21,39]. We measured three-pulse echo decays as a function of t_{23}, with t_{12} fixed at 0.3 μs, as shown in Fig. 3(a). The initial fast decay is from spectral diffusion while the slower decay results from population relaxation.

Both two- and three-pulse echoes can be modeled by a time-dependent effective homogeneous linewidth Γ_{eff} [21] and echo amplitude

$$A(t_{12}, t_{23}) = A_0 e^{(-t_{23}/T_{1e})} e^{[-2t_{12}\pi\Gamma_{\mathrm{eff}}(t_{12},t_{23})]}, \quad (2)$$

where T_{1e} corresponds to the population relaxation time. Contributions to Γ_{eff} arise from ground-state Er^{3+} spins at both sites in the lattice. Because of the narrow optical excitation bandwidth, the excited-state ion concentration is $\sim 10^3$ times lower than the ground-state concentration and can be neglected. For our conditions, site 2 spins rapidly relax by mutual spin flip-flop processes (spin diffusion) due to their large ground state effective g factor of 14. A simple theoretical estimate (see the Supplemental Material [30]) shows that this causes decoherence over sub-μs timescales, resulting in a width Γ_0 that is independent of t_{23} and t_{12}. Er^{3+} spins in site 1 have a g factor of 4, and their flip-flop rate R_{ff} is roughly $(14/4)^4 = 150$ times smaller than that of site 2 spins. This slower relaxation produces a spectral diffusion of Γ_{eff} given by Ref. [21]

$$\Gamma_{\mathrm{eff}}(t_{12}, t_{23}) = \Gamma_0 + \frac{1}{2}\Gamma_{\mathrm{SD}}(Rt_{12} + 1 - e^{-Rt_{23}}), \quad (3)$$

where R is the site 1 spin relaxation rate and Γ_{SD} is the distribution of interaction strengths between resonant spins and other site 1 spins in the environment.

The two- and three-pulse echo decays were recorded between 1.6 and 3.5 K and fitted to Eqs. (2) and (3) using a rate R including a two-phonon Orbach term combined with the flip-flop rate R_{ff} for site 1. An example fitted curve is shown in Fig. 3(a) for $T = 2.5$ K. The fits gave values of $\Gamma_0 = 2.7 \times 10^5$ Hz, $\Gamma_{\mathrm{SD}} = 4.3 \times 10^5$ Hz, $R_{\mathrm{ff}} = 2.1 \times 10^4$ s^{-1}, which compare well with theoretical calculations (see the Supplemental Material [30]). Reasonable agreement was also found between two-pulse echo T_{2e} values fitted to experimental data using Eq. (1) and those calculated from the fit parameters [see Fig. 3(b)]. T_{1e} values were determined from the fits and were explained by the sum of optical excitation and emission rates combined with an Orbach process (see Fig. 3(b) and the Supplemental Material [30]). At the lowest temperatures, T_{1e} reached 1.2 ms, limited by optical stimulated emission due to continuous excitation by the laser. In a pulsed configuration without laser excitation during the echo sequence, T_{1e} would increase to $T_{1,\mathrm{opt}} = 8$ ms [40].

For our conditions, T_{2e} is limited by decoherence from relaxation of ground-state spins. This decoherence would be reduced at lower temperatures since the Orbach contribution rapidly decreases as $\exp(-\Delta_g/T)$, while flip-flop rates decrease as $[\mathrm{sech}(g_g\mu_B B/2kT)]^2$, where k is the Boltzmann factor. For example, consider a weak field of 50 mT that is compatible with superconducting resonators and where the excited-state splitting is ~ 2 GHz, in the range of typical microwave photons. At a temperature of 20 mK, decoherence only results from site 1 ground-state spin flip-flops because site 2 spins, with their large g factor, are completely polarized. The site 1 flip-flop rate R_{ff} would be reduced by a factor of ~ 350 compared to 2 K. Together, these effects would increase the excited-state spin coherence lifetime to $T_{2e} \approx 2.9$ ms (see the Supplemental Material [30]). This is likely to approach the decoherence limit due to ^{89}Y spin flips [21]. In contrast, even at very low temperatures, site 1 ground-state excitations will experience rapid decoherence through the flip-flop process due to the large number of other resonant spins present in the lattice. In fact, spins excited into the higher energy spin state will have an increasing number of neighbors in the lower energy spin state to flip-flop with as the temperature is decreased, accelerating decoherence to as much as twice the high-temperature rate. For our system, this effect limits T_{2g} to less than 48 μs even at the lowest temperatures (see the Supplemental Material [30]). Moreover, a rephasing control pulse applied over the entire spin linewidth would cause strong ISD, further reducing T_{2g} to ~ 1 μs, independent of temperature. This effect can explain why we did not observe any ground-state spin echo for the conditions used in the excited-state measurements, as well as why long electron-spin coherence times have been difficult to achieve with ground-state spin transduction protocols. For example, our analysis is in qualitative agreement with the ground-state site 2 coherence lifetime of 5.6 μs observed at 30 mK with a different magnetic field orientation [20].

Finally, we outline an excited-state scheme for optical to microwave transduction. Previous proposals used the ground-state spin by coupling it off-resonantly [15] or resonantly [16] to a microwave cavity. One limiting factor for efficient conversion in [16] is the short coherence lifetime compared to the coupling strength.

To employ the excited state for transduction, the protocol from Ref. [16] can be modified as follows. The first step is the same as in Ref. [16]; we prepare a narrow spectral feature and then apply a magnetic field gradient to produce an inhomogeneously broadened feature. An incoming optical photon is then absorbed on the $|1\rangle$–$|4\rangle$ transition. The induced inhomogeneous broadening and free evolution of the system cause dephasing of the optical coherence, preventing re-emission and ensuring that the optical photon is stored. In the next step, a series of π pulses are applied on the $|1\rangle$–$|3\rangle$ transition. This is different from the original protocol, where the π pulses were applied on the $|2\rangle$–$|4\rangle$ transition. The first π pulse brings the population from state $|1\rangle$ to $|3\rangle$ and subsequent free evolution further dephases the system due to the spin inhomogeneous broadening, but at a possibly different rate. After a delay, we apply a second π pulse to bring population back into $|1\rangle$, while simultaneously reversing the field gradient to begin the rephasing procedure. Since spontaneously emitted photons will have a different frequency than converted photons, inverting the population on the optical transition does not introduce photon noise at the converted frequency. Once dephasing due to inhomogeneous broadening of the excited state is compensated, we apply another π pulse, moving population

to state $|3\rangle$ to complete the rephasing. This procedure compensates for dynamical phases induced by the field gradient. To further compensate for dephasing due to intrinsic spin inhomogeneous broadening, a sequence of dynamical decoupling microwave pulses could be applied on the $|3\rangle$–$|4\rangle$ transition. After successful rephasing, the system is in a state that strongly couples to a microwave cavity due to collective enhancement of the coupling strength, allowing for efficient transfer of the matter excitation to a microwave photon. Assuming the same spin-cavity coupling strength of $v/2\pi = 34$ MHz as in Ref. [20], which is justified since the principal values of the magnetic g tensors for the $^4I_{15/2}$ and $^4I_{13/2}$ states in Er^{3+}: Y_2SiO_5 are roughly the same [38], and using our measured spin coherence lifetime of $T_{2e} = 1.6$ μs, we can estimate the transfer efficiency of the spin excitation to a microwave photon to be $\eta \approx \exp(-\pi/2/T_{2e}v) \approx 99\%$. To obtain the overall conversion efficiency, we must combine this with the efficiency of mapping the optical photon to the spin excitation, which can be highly efficient provided a large optical depth [41] (for quantitative analysis of the effect of optical density on efficiency, see Ref. [42]); however, we note that in an actual experiment, other implementation factors, such as imperfections in optical pumping or pi pulses, might cause diminishing increases in efficiency.

A further advantage of using excited-state spin transitions is that only ions in the laser beam cross section interact with the microwave cavity, making spatial hole burning, as required in the original protocol, unnecessary. Also, reversing the protocol allows conversion of a microwave photon to a propagating telecom photon. Moreover, the optical photon's bandwidth can be tuned, as in the original protocol, by controlling the strength of the field gradient.

In conclusion, we observed electron spin echoes in the optically excited state of an erbium-doped crystal. Coherence lifetimes of up to 1.6 μs were recorded for a field of 8.7 mT at 1.9 K, and analysis of the decoherence processes suggest that ms lifetimes should be reached under conditions used for superconducting qubits. We propose a scheme to exploit these long coherence lifetimes for reversible optical to microwave conversion, with our analysis predicting near unity conversion efficiency. Overall, using excited-state spin transitions opens a new and attractive way to coherently interface RE ensembles with microwave cavities and may stimulate new proposals for transducer devices.

We thank J. G. Bartholomew, N. Sinclair, M. Falamarzi, D. Oblak, and W. Tittel for useful discussions, and A. Marsh and R. Nerem for assistance during measurements. This work received funding from the joint French-U.S. Agence Nationale de la Recherche project (Grant No. 14-CE26-0037-01) and U.S. National Science Foundation Grant No. CHE-1416454, as well as Nano'K project Rare Earth Doped Crystals for Ultra-High Stability, the University of Calgary, and Natural Sciences and Engineering Research Council of Canada.

Note added.—A related experiment using hyperfine states of $^{167}Er^{3+}$ has been performed in parallel [43].

[1] C. W. Thiel, T. Böttger, and R. L. Cone, J. Lumin. **131**, 353 (2011).
[2] P. Goldner, A. Ferrier, and O. Guillot-Noël, in *Handbook on the Physics and Chemistry of Rare Earths*, edited by J.-C. G. Bünzli and V. K. Pecharsky (Elsevier, Amsterdam, 2015), Vol. 46, pp. 1–78.
[3] M. Zhong, M. P. Hedges, R. L. Ahlefeldt, J. G. Bartholomew, S. E. Beavan, S. M. Wittig, J. J. Longdell, and M. J. Sellars, Nature (London) **517**, 177 (2015).
[4] C. Laplane, P. Jobez, J. Etesse, N. Gisin, and M. Afzelius, Phys. Rev. Lett. **118**, 210501 (2017).
[5] C. Clausen, I. Usmani, F. Bussières, N. Sangouard, M. Afzelius, H. de Riedmatten, and N. Gisin, Nature (London) **469**, 508 (2011).
[6] F. Bussières, C. Clausen, A. Tiranov, B. Korzh, V. B. Verma, S. W. Nam, F. Marsili, A. Ferrier, P. Goldner, H. Herrmann, C. Silberhorn, W. Sohler, M. Afzelius, and N. Gisin, Nat. Photonics **8**, 775 (2014).
[7] N. Maring, P. Farrera, K. Kutluer, M. Mazzera, G. Heinze, and H. de Riedmatten, Nature (London) **551**, 485 (2017).
[8] M. Bonarota, J.-L. Le Gouët, and T. Chanelière, New J. Phys. **13**, 013013 (2011).
[9] N. Sinclair, E. Saglamyurek, H. Mallahzadeh, J. A. Slater, M. George, R. Ricken, M. P. Hedges, D. Oblak, C. Simon, W. Sohler, and W. Tittel, Phys. Rev. Lett. **113**, 053603 (2014).
[10] M. P. Hedges, J. J. Longdell, Y. Li, and M. J. Sellars, Nature (London) **465**, 1052 (2010).
[11] M. Sabooni, Q. Li, S. Kröll, and L. Rippe, Phys. Rev. Lett. **110**, 133604 (2013).
[12] E. Saglamyurek, N. Sinclair, J. A. Slater, K. Heshami, D. Oblak, and W. Tittel, New J. Phys. **16**, 065019 (2014).
[13] J. G. Bartholomew, K. de Oliveira Lima, A. Ferrier, and P. Goldner, Nano Lett. **17**, 778 (2017).
[14] T. Zhong, J. M. Kindem, J. G. Bartholomew, J. Rochman, I. Craiciu, E. Miyazono, M. Bettinelli, E. Cavalli, V. Verma, S. W. Nam, F. Marsili, M. D. Shaw, A. D. Beyer, and A. Faraon, Science **357**, 1392 (2017).
[15] L. A. Williamson, Y. H. Chen, and J. J. Longdell, Phys. Rev. Lett. **113**, 203601 (2014).
[16] C. O'Brien, N. Lauk, S. Blum, G. Morigi, and M. Fleischhauer, Phys. Rev. Lett. **113**, 063603 (2014).
[17] X. Fernandez-Gonzalvo, Y. H. Chen, C. Yin, S. Rogge, and J. J. Longdell, Phys. Rev. A **92**, 062313 (2015).
[18] Y. H. Chen, X. Fernandez-Gonzalvo, and J. J. Longdell, Phys. Rev. B **94**, 075117 (2016).
[19] S. Probst, H. Rotzinger, A. V. Ustinov, and P. A. Bushev, Phys. Rev. B **92**, 014421 (2015).
[20] S. Probst, H. Rotzinger, S. Wünsch, P. Jung, M. Jerger, M. Siegel, A. V. Ustinov, and P. A. Bushev, Phys. Rev. Lett. **110**, 157001 (2013).

[21] T. Böttger, C. W. Thiel, Y. Sun, and R. L. Cone, Phys. Rev. B **73**, 075101 (2006).
[22] E. Z. Cruzeiro, A. Tiranov, I. Usmani, C. Laplane, J. Lavoie, A. Ferrier, P. Goldner, N. Gisin, and M. Afzelius, Phys. Rev. B **95**, 205119 (2017).
[23] B. Herzog and E. L. Hahn, Phys. Rev. **103**, 148 (1956).
[24] C. W. Thiel, R. M. Macfarlane, Y. Sun, T. Böttger, N. Sinclair, W. Tittel, and R. L. Cone, Laser Phys. **24**, 106002 (2014).
[25] E. Zambrini Cruzeiro, A. Tiranov, J. Lavoie, A. Ferrier, P. Goldner, N. Gisin, and M. Afzelius, New J. Phys. **20**, 053013 (2018).
[26] T. Böttger, C. W. Thiel, Y. Sun, and R. L. Cone, Phys. Rev. B **74**, 075107 (2006).
[27] E. Saglamyurek, T. Lutz, L. Veissier, M. P. Hedges, C. W. Thiel, R. L. Cone, and W. Tittel, Nat. Photonics **9**, 83 (2015).
[28] J. Mlynek, N. C. Wong, R. G. DeVoe, E. S. Kintzer, and R. G. Brewer, Phys. Rev. Lett. **50**, 993 (1983).
[29] C. Li, C. Wyon, and R. Moncorgé, IEEE J. Quantum Electron. **28**, 1209 (1992).
[30] See Supplemental Material at http://link.aps.org/supplemental/10.1103/PhysRevLett.122.247401 for further details on experimental conditions and apparatus, additional spin echo data and theoretical models, which also includes Refs. [31–36].
[31] R. C. Hilborn, Am. J. Phys. **50**, 982 (1982).
[32] B. A. Young and H. J. Stapleton, Phys. Lett. **21**, 498 (1966).
[33] G. Wolfowicz, H. Maier-Flaig, R. Marino, A. Ferrier, H. Vezin, J. J. L. Morton, and P. Goldner, Phys. Rev. Lett. **114**, 170503 (2015).
[34] T. Böttger, C. W. Thiel, R. L. Cone, Y. Sun, and A. Faraon, Phys. Rev. B **94**, 045134 (2016).
[35] H.-J. Lim, S. Welinski, A. Ferrier, P. Goldner, and J. J. L. Morton, Phys. Rev. B **97**, 064409 (2018).
[36] R. M. Macfarlane, R. Wannemacher, D. Boye, Y. P. Wang, and R. S. Meltzer, J. Lumin. **48–49**, 313 (1991).
[37] O. Guillot-Noël, P. Goldner, Y. L. Du, E. Baldit, P. Monnier, and K. Bencheikh, Phys. Rev. B **74**, 214409 (2006).
[38] Y. Sun, T. Böttger, C. W. Thiel, and R. L. Cone, Phys. Rev. B **77**, 085124 (2008).
[39] W. Mims, Phys. Rev. **168**, 370 (1968).
[40] C. W. Thiel, W. R. Babbitt, and R. L. Cone, Phys. Rev. B **85**, 174302 (2012).
[41] B. Kraus, W. Tittel, N. Gisin, M. Nilsson, S. Kröll, and J. I. Cirac, Phys. Rev. A **73**, 020302(R) (2006).
[42] N. Sangouard, C. Simon, M. Afzelius, and N. Gisin, Phys. Rev. A **75**, 032327 (2007).
[43] J. V. Rakonjac, Y.-H. Chen, S. P. Horvath, and J. J. Longdell, arXiv:1802.03862.